NONLINEAR OBSERVER FOR NONLINEAR ADAPTIVE GUIDANCE LAW CONSIDERING TARGET UNCERTAINTIES AND CONTROL LOOP DYNAMICS

DongKyoung Chwa*, A.G. Sreenatha*, Ki Hong Im†, Jin Young Choi†, and Jin H. Seo †

*School of Aerospace, Civil, and Mechanical Engineering,
UNSW@ADFA (The University of New South Wales at Australian Defence Force Academy), Australia
e-mail: dkchwa@neuro.snu.ac.kr
Fax : +82-2-883-3251

†School of Electrical Engineering, Seoul National University, Korea

Keywords: nonlinear observer, nonlinear adaptive guidance, target maneuver, control loop dynamics, integrated guidance and control model.

Abstract

This paper proposes a nonlinear observer design method for nonlinear adaptive guidance. Several states of the previously proposed nonlinear adaptive guidance law are estimated by a nonlinear observer, which is designed based on the integrated guidance and control model. Using the estimated states and uncertainties, desired engagement performance of the nonlinear adaptive guidance law can be obtained against target maneuver and the limited performance of control loop. The performance and stability analyses of the proposed observer and simulations are included to demonstrate the practical application of our scheme.

1 Introduction

There has been much research on guidance area [13, 6] including proportional navigation (PN), true proportional navigation (TPN), augmented proportional navigation (APN), optimal guidance law (OGL), nonlinear guidance laws using Lyapunov method [14], nonlinear geometric method [2,9,10], nonlinear H_∞ method [15], and sliding mode guidance (SM) [3,1,16].

All the above guidance laws, however, do not consider the actual dynamics of missile control systems and have limitation in their performance of the overall guidance and control loop. Accordingly, the integrated guidance and control approach is suggested in [12,8,11], where the optimal control technique together with gain scheduling approach is used. In [4], another approach to integrated guidance and control is suggested including the actual missile control loop in [7]. That is, an integrated guidance and control loop, which is valid for all flight conditions and also includes the uncertainties in both control loop dynamics and target acceleration, is formulated and then a nonlinear adaptive guidance law is designed. This approach is shown to achieve better interception performance than PN guidance. This, however, assumes that all states in the guidance law are available.

In this paper, a nonlinear observer is proposed for the nonlinear adaptive guidance law based on integrated guidance and control model in [4]. First, the integrated guidance and control model is re-formulated as a normal form with respect to available states by considering unavailable information as parametric and non-parametric uncertainties. Then, a nonlinear observer is designed and the estimated states and uncertainties are used in the nonlinear adaptive guidance law. The performance and stability of the proposed adaptive observer are analyzed and simulation results are also performed to demonstrate the proposed approach.

2 Integrated guidance and control model

In this section, an integrated model for guidance and control loop proposed in [4] is reviewed, and then it is further re-formulated for the design of nonlinear observer.

First, using the controller in [7], [4] shows that the control loop consisting of the nonlinear controller and missile dynamics has output response given by

$$\ddot{a}_m + 2\xi\omega_n a_m + \omega_n^2 a_m = \omega_n^2 a_{mc} + \Delta_c \tag{1}$$

where a_{mc} is acceleration command; a_m is acceleration output; ξ and ω_n are design parameters of the control loop; and Δ_c is a bounded uncertainty. Equation (1) can be expressed as

$$\begin{aligned}\dot{X}_c &= \begin{pmatrix} 0 & 1 \\ -a_{c1} & -a_{c2} \end{pmatrix} X_c + \begin{pmatrix} 0 \\ b_c \end{pmatrix} u_c + \begin{pmatrix} 0 \\ \Delta_c \end{pmatrix} \\ &=: A_c X_c + B_c u_c + D_c \end{aligned} \tag{2}$$

where $X_c = (x_{c1} \quad x_{c2})^T = (a_m \quad \dot{a}_m)^T$, $a_{c1} = \omega_n^2$, $a_{c2} = 2\xi\omega_n$, $b_c = \omega_n^2$, and $u_c = a_{mc}$.

Secondly, [4] shows that the state equation of the guidance loop can be expressed by

$$
\begin{aligned}
\dot{X}_g &= \begin{pmatrix} 0 & 1 \\ -a_{g1}(t) & -a_{g2}(t) \end{pmatrix} X_g + \begin{pmatrix} 0 \\ -b_g(t) \end{pmatrix} a_m + \begin{pmatrix} 0 \\ b_g(t) \end{pmatrix} a_T \\
&=: A_g X_g + B_g u_g + D_g
\end{aligned} \tag{3}
$$

where $X_g = (x_{g1} \quad x_{g2})^T = (\sigma \quad \dot{\sigma})^T$; σ is a line-of-sight (LOS) angle; $a_{g1}(t) = \ddot{R}(t)/R(t)$, $a_{g2}(t) = 2\dot{R}(t)/R(t)$, $b_g(t) = 1/R(t)$; a_T is target acceleration; $u_g = a_m$; and R , $\dot{R}$ are the relative distance and velocity between the target and the missile. Since from Equation (2) $u_g = x_{c1} = C_g X_c$ holds for $C_g := [1 \quad 0]$, the control loop in Equation (2) and the guidance loop in Equation (3) can be combined as

$$
\begin{aligned}
\dot{X}_{igc} &= \begin{pmatrix} A_g & B_g C_g \\ 0 & A_c \end{pmatrix} X_{igc} + \begin{pmatrix} 0 \\ B_c \end{pmatrix} u_c + \begin{pmatrix} D_g \\ D_c \end{pmatrix} \\
&= A_{igc} X_{igc} + B_{igc} u_c + D_{igc}
\end{aligned} \tag{4a}
$$

$$
\begin{aligned}
Y_{igc} &= x_{g2} \\
&= C_{igc} X_{igc}
\end{aligned} \tag{4b}
$$

where

$$
X_{igc} = \begin{pmatrix} X_g \\ X_c \end{pmatrix}, \; A_{igc} = \begin{pmatrix} 0 & 1 & 0 & 0 \\ -a_{g1} & -a_{g2} & -b_g & 0 \\ 0 & 0 & 0 & 1 \\ 0 & 0 & -a_{c1} & -a_{c2} \end{pmatrix},
$$

$$
B_{igc} = \begin{pmatrix} 0 & 0 & 0 & b_c \end{pmatrix}^T, C_{igc} = (0 \quad 1 \quad 0 \quad 0),
$$

$$
D_{igc} = (0 \quad b_g a_T \quad 0 \quad \Delta_c)^T .
$$

In [4], the guidance law is designed by deriving an integrated guidance and control model from Equation (4). However, all parameters in Equation (4) are not available. While a_{c1}, a_{c2} in A_{igc} of Equation (4) are available since they are design parameters of the control loop, a_{g1}, a_{g2}, b_g are decomposed into known parts $\hat{a}_{g1}$, $\hat{a}_{g2}$, $\hat{b}_g$ and unknown parts $\tilde{a}_{g1}$, $\tilde{a}_{g2}$, $\tilde{b}_g$ such as

$$
a_{g1} = \hat{a}_{g1} + \tilde{a}_{g1} \tag{5a}
$$

$$
a_{g2} = \hat{a}_{g2} + \tilde{a}_{g2} \tag{5b}
$$

$$
b_g = \hat{b}_g + \tilde{b}_g . \tag{5c}
$$

For easier application, a normal form of integrated guidance and control model with uncertainties is formulated in the following.

In proportional navigation, acceleration commands are generated to make the rate of rotation of the LOS (line-of-sight) be zero and this guarantees the interception performance. So, the output is chosen by

$$
y = Y_{igc} =: x_1 \tag{6}
$$

as in [16], which will be made to be zero by the guidance law. Differentiating the output, we have

$$
\begin{aligned}
\dot{x}_1 &= -a_{g1} x_{g1} - a_{g2} x_1 - b_g x_{c1} + b_g a_T \\
&= x_2 + \theta_1^T \varphi_1 + \Delta_1
\end{aligned} \tag{7}
$$

where

$$
x_2 = -\hat{a}_{g1} x_{g1} - \hat{a}_{g2} x_1 - \hat{b}_g x_{c1} ,
$$

$$
\theta_1^T = [\theta_{11} \quad \theta_{12} \quad \theta_{13}]^T = [-\tilde{a}_{g1} \quad -\tilde{a}_{g2} \quad -\tilde{b}_g]
$$

$$
\varphi_1^T = [x_{g1} \quad x_1 \quad x_{c1}], \; \Delta_1 = b_g a_T .
$$

In the same way, we can have

$$
\begin{aligned}
\dot{x}_2 &= -\dot{\hat{a}}_{g1} x_{g1} - \hat{a}_{g1} \dot{x}_{g1} - \dot{\hat{a}}_{g2} x_1 - \hat{a}_{g2} \dot{x}_1 - \dot{\hat{b}}_g x_{c1} - \hat{b}_g \dot{x}_{c1} \\
&= -\dot{\hat{a}}_{g1} x_{g1} - \hat{a}_{g1} x_1 - \dot{\hat{a}}_{g2} x_1 - \hat{a}_{g2} (x_2 + \theta_1^T \varphi_1 + \Delta_1) \\
&\quad - \dot{\hat{b}}_g x_{c1} - \hat{b}_g x_{c2} \\
&= -\hat{a}_{g1} x_1 - \hat{a}_{g2} x_2 - \hat{b}_g x_{c2} - \hat{a}_{g2} \theta_1^T \varphi_1 - \dot{\hat{a}}_{g1} x_{g1} - \dot{\hat{a}}_{g2} x_1 \\
&\quad - \dot{\hat{b}}_g x_{c1} - \hat{a}_{g2} \Delta_1 \\
&= x_3 + \theta_2^T \varphi_2 + \Delta_2
\end{aligned} \tag{8}
$$

where

$$
x_3 = -\hat{a}_{g1} x_1 - \hat{a}_{g2} x_2 - \hat{b}_g x_{c2}
$$

$$
\begin{aligned}
\theta_2^T &= [\theta_{21} \quad \theta_{22} \quad \theta_{23}]^T \\
&= [-\hat{a}_{g2} \theta_{11} - \dot{\hat{a}}_{g1} \quad -\hat{a}_{g2} \theta_{12} - \dot{\hat{a}}_{g2} \quad -\hat{a}_{g2} \theta_{13} - \dot{\hat{b}}_g]
\end{aligned}
$$

$$
\varphi_2^T = [x_{g1} \quad x_1 \quad x_{c1}], \; \Delta_2 = -\hat{a}_{g2} \Delta_1
$$

and

$$
\begin{aligned}
\dot{x}_3 &= -\dot{\hat{a}}_{g1} x_1 - \hat{a}_{g1} \dot{x}_1 - \dot{\hat{a}}_{g2} x_2 - \hat{a}_{g2} \dot{x}_2 - \dot{\hat{b}}_g x_{c2} - \hat{b}_g \dot{x}_{c2} \\
&= -\dot{\hat{a}}_{g1} x_1 - \hat{a}_{g1} (x_2 + \theta_1^T \varphi_1 + \Delta_1) - \dot{\hat{a}}_{g2} x_2 - \hat{a}_{g2} (x_3 + \theta_2^T \varphi_2 \\
&\quad + \Delta_2) - \dot{\hat{b}}_g x_{c2} - \hat{b}_g (-a_{c1} x_{c1} - a_{c2} x_{c2} + b_c u_c + \Delta_c) \\
&= -\hat{a}_{g1} x_2 - \hat{a}_{g2} x_3 - \hat{b}_g (-a_{c1} x_{c1} - a_{c2} x_{c2} + b_c u_c) - \hat{a}_{g1} \theta_1^T \varphi_1 \\
&\quad - \hat{a}_{g2} \theta_2^T \varphi_2 - \dot{\hat{a}}_{g1} x_1 - \dot{\hat{a}}_{g2} x_2 - \dot{\hat{b}}_g x_{c2} - \hat{a}_{g1} \Delta_1 - \hat{a}_{g2} \Delta_2 - \hat{b}_g \Delta_c \\
&= -\hat{a}_{g1} x_2 - \hat{a}_{g2} x_3 + \hat{b}_g a_{c1} x_{c1} + \hat{b}_g a_{c2} x_{c2} - \hat{b}_g b_c u_c + \theta_3^T \varphi_3 + \Delta_3
\end{aligned} \tag{9}
$$

where

$$\theta_3^T = [\theta_{31} \quad \theta_{32} \quad \theta_{33} \quad \theta_{34} \quad \theta_{35}]^T$$
$$= [(-\hat{a}_{g1}\theta_{11} - \hat{a}_{g2}\theta_{21}),\ (-\hat{a}_{g1}\theta_{12} - \hat{a}_{g2}\theta_{22} - \dot{\hat{a}}_{g1}),\ -\dot{\hat{a}}_{g2},$$
$$(-\hat{a}_{g1}\theta_{13} - \hat{a}_{g2}\theta_{23}),\ -\dot{\hat{b}}_g\,]$$
$$\varphi_3^T = [x_{g1} \quad x_1 \quad x_2 \quad x_{c1} \quad x_{c2}\,],$$
$$\Delta_3 = -\hat{a}_{g1}\Delta_1 - \hat{a}_{g2}\Delta_2 - \hat{b}_g\Delta_c\ .$$

Thus, an integrated guidance and control model with uncertainties can be described by

$$\dot{X} = \begin{pmatrix} 0 & 1 & 0 \\ 0 & 0 & 1 \\ 0 & 0 & 0 \end{pmatrix} X + \begin{pmatrix} 0 \\ 0 \\ -\hat{b}_g b_c \end{pmatrix} u_c + \begin{pmatrix} 0 \\ 0 \\ -\hat{a}_{g1}x_2 - \hat{a}_{g2}x_3 + \hat{b}_g a_{c1}x_{c1} + \hat{b}_g a_{c2}x_{c2} \end{pmatrix} + \begin{pmatrix} \theta_1^T\varphi_1 \\ \theta_2^T\varphi_2 \\ \theta_3^T\varphi_3 \end{pmatrix} + \begin{pmatrix} \Delta_1 \\ \Delta_2 \\ \Delta_3 \end{pmatrix} \tag{10a}$$

$$y = x_1 \tag{10b}$$

where $X = [x_1 \quad x_2 \quad x_3]^T$.

3 Nonlinear observer based on integrated guidance and control model

In this section, a nonlinear observer is designed for the integrated guidance and control model under the following assumption.

Assumption 3.1: θ_i and Δ_i are bounded as $|\theta_i| := [|\theta_{i1}|, \ \cdots, \ |\theta_{ij}|] \le \mu_i := [\mu_{i1}, \ \cdots, \ \mu_{ij}]$, and $|\Delta_i| \le D_i$ where $1 \le i \le 3$ and $3 \le j \le 5$.

The proposed observer is given by

$$\dot{\hat{X}} = \begin{pmatrix} 0 & 1 & 0 \\ 0 & 0 & 1 \\ 0 & 0 & 0 \end{pmatrix} \hat{X} + \begin{pmatrix} k_1 \\ k_2 \\ k_3 \end{pmatrix} \varepsilon + \begin{pmatrix} m_1\tilde{x}_1 \\ m_2\tilde{x}_2 \\ m_3\tilde{x}_3 \end{pmatrix} + \begin{pmatrix} 0 \\ 0 \\ -\hat{b}_g b_c \end{pmatrix} u_c + \begin{pmatrix} 0 \\ 0 \\ -\hat{a}_{g1}x_2 - \hat{a}_{g2}x_3 + \hat{b}_g a_{c1}x_{c1} + \hat{b}_g a_{c2}x_{c2} \end{pmatrix} + \begin{pmatrix} (\hat{\mu}_1^T|\varphi_1| + \hat{D}_1)\mathrm{sgn}(\tilde{x}_1) \\ (\hat{\mu}_2^T|\varphi_2| + \hat{D}_2)\mathrm{sgn}(\tilde{x}_2) \\ (\hat{\mu}_3^T|\varphi_3| + \hat{D}_3)\mathrm{sgn}(\tilde{x}_3) \end{pmatrix} \tag{11}$$

and the adaptation law by

$$\dot{\hat{\mu}}_{ij} = \gamma_{\mu i}|\tilde{x}_i| \cdot |\varphi_{ij}|\ ,\ \dot{\hat{D}}_i = \gamma_{Di}|\tilde{x}_i| \tag{12}$$

where $\hat{X} = [\hat{x}_1 \quad \hat{x}_2 \quad \hat{x}_3]$; ε is obtained from $\dot{\varepsilon} = -a_0\varepsilon + a_0\tilde{x}_1$ with a positive constant a_0 ; $\hat{\mu}_i = [\hat{\mu}_{i1}, \ \cdots, \ \hat{\mu}_{ij}]$ and $\hat{D}_i$ are estimates of μ_i and D_i , $|\varphi_i| := [|\varphi_{i1}|, \ \cdots, \ |\varphi_{ij}|]^T$, and $\gamma_{\mu i}$ and γ_{Di} are parameter adaptation gains where $1 \le i \le 3$ and $3 \le j \le 5$; and $k_i, m_i > 0$ are chosen such that a positive definite matrix $P = diag(P_1, P_2, P_3, P_4)$ and a positive definite matrix Q exist satisfying $A^T P + PA = -Q$ for

$$A = \begin{pmatrix} -m_1 & 1 & 0 & -k_1 \\ 0 & -m_2 & 1 & -k_2 \\ 0 & 0 & -m_3 & -k_3 \\ a_0 & 0 & 0 & -a_0 \end{pmatrix}.$$

It should be noted that a diagonal matrix P exists for this type of matrix A .

Here, we define $E = [\tilde{X} \quad \varepsilon]^T \in R^{4\times 1}$ and estimation errors $\tilde{X} = X - \hat{X}$, $\tilde{x}_i = x_i - \hat{x}_i$, $\tilde{\mu}_i = \mu_i - \hat{\mu}_i$, and $\tilde{D}_i = D_i - \hat{D}_i$ for $1 \le i \le 3$. We further make the following assumption.

Assumption 3.2: States φ_i , $1 \le i \le 3$, are bounded.

Then, stability and performance for the above observer is shown in the following theorem.

Theorem 3.1 (Nonlinear Observer)

The state estimation errors between the actual states of the integrated guidance and control model (10) and the estimated ones by the nonlinear observer (11) and the adaptive law (12) under Assumption 3.1 are stable in the sense that for $1 \le i \le 3$

1. $\tilde{\mu}_i, \hat{\mu}_i, \tilde{D}_i, \hat{D}_i \in L_\infty$,
2. $E \in L_2 \cap L_\infty$.

Furthermore, when Assumption 3.2 holds as well, we can have

3. $\dot{\hat{\mu}}_i, \dot{\hat{D}}_i \in L_2 \cap L_\infty$,
4. $\dot{E} \in L_\infty$,
5. E , $\dot{\hat{\mu}}_i$, and $\dot{\hat{D}}_i$ converge to zero asymptotically .

Proof: From Equations (10a) and (11), we have

$$\frac{d}{dt}E = AE + \begin{pmatrix} \theta_1^T\varphi_1 \\ \theta_2^T\varphi_2 \\ \theta_3^T\varphi_3 \\ 0 \end{pmatrix} + \begin{pmatrix} \Delta_1 \\ \Delta_2 \\ \Delta_3 \\ 0 \end{pmatrix} - \begin{pmatrix} (\hat{\mu}_1^T|\varphi_1| + \hat{D}_1)\,\mathrm{sgn}(\tilde{x}_1) \\ (\hat{\mu}_2^T|\varphi_2| + \hat{D}_2)\,\mathrm{sgn}(\tilde{x}_2) \\ (\hat{\mu}_3^T|\varphi_3| + \hat{D}_3)\,\mathrm{sgn}(\tilde{x}_3) \\ 0 \end{pmatrix}.$$

We choose a Lyapunov function

$$V = \frac{1}{2} E^T P\, E + \sum_{i=1}^{3} \frac{P_i}{2} \left(\frac{\tilde{\mu}_i^T \tilde{\mu}_i}{\gamma_{\mu i}} + \frac{\tilde{D}_i^2}{\gamma_{Di}} \right)$$

for $P = diag(P_1, P_2, P_3, P_4) > 0$ and take its time derivative to have

$$\begin{aligned}
\dot{V} &= \frac{1}{2} E^T (A^T P + PA) E \\
&\quad + E^T P \left\{ \begin{pmatrix} \theta_1^T \varphi_1 \\ \theta_2^T \varphi_2 \\ \theta_3^T \varphi_3 \\ 0 \end{pmatrix} + \begin{pmatrix} \Delta_1 \\ \Delta_2 \\ \Delta_3 \\ 0 \end{pmatrix} - \begin{pmatrix} (\hat{\mu}_1^T |\varphi_1| + \hat{D}_1)\operatorname{sgn}(\tilde{x}_1) \\ (\hat{\mu}_2^T |\varphi_2| + \hat{D}_2)\operatorname{sgn}(\tilde{x}_2) \\ (\hat{\mu}_3^T |\varphi_3| + \hat{D}_3)\operatorname{sgn}(\tilde{x}_3) \\ 0 \end{pmatrix} \right\} \\
&\quad + \sum_{i=1}^{3} P_i \left(\frac{\tilde{\mu}_i^T \dot{\tilde{\mu}}_i}{\gamma_{\mu i}} + \frac{\tilde{D}_i \dot{\tilde{D}}_i}{\gamma_{Di}} \right) \\
&\le -\frac{1}{2} E^T Q\, E + \begin{pmatrix} |\tilde{x}_1| \\ |\tilde{x}_2| \\ |\tilde{x}_3| \\ |\varepsilon| \end{pmatrix}^T P \left\{ \begin{pmatrix} \mu_1^T |\varphi_1| \\ \mu_2^T |\varphi_2| \\ \mu_3^T |\varphi_3| \\ 0 \end{pmatrix} + \begin{pmatrix} D_1 \\ D_2 \\ D_3 \\ 0 \end{pmatrix} - \begin{pmatrix} \hat{\mu}_1^T |\varphi_1| + \hat{D}_1 \\ \hat{\mu}_2^T |\varphi_2| + \hat{D}_2 \\ \hat{\mu}_3^T |\varphi_3| + \hat{D}_3 \\ 0 \end{pmatrix} \right\} \\
&\quad + \sum_{i=1}^{3} P_i \left(\frac{\tilde{\mu}_i^T \dot{\tilde{\mu}}_i}{\gamma_{\mu i}} + \frac{\tilde{D}_i \dot{\tilde{D}}_i}{\gamma_{Di}} \right) \\
&\le -\frac{1}{2} E^T Q\, E + \begin{pmatrix} |\tilde{x}_1| \\ |\tilde{x}_2| \\ |\tilde{x}_3| \\ |\varepsilon| \end{pmatrix}^T P \begin{pmatrix} \tilde{\mu}_1^T |\varphi_1| + \tilde{D}_1 \\ \tilde{\mu}_2^T |\varphi_2| + \tilde{D}_2 \\ \tilde{\mu}_3^T |\varphi_3| + \tilde{D}_3 \\ 0 \end{pmatrix} \\
&\quad + \sum_{i=1}^{3} P_i \left(\frac{\tilde{\mu}_i^T \dot{\tilde{\mu}}_i}{\gamma_{\mu i}} + \frac{\tilde{D}_i \dot{\tilde{D}}_i}{\gamma_{Di}} \right) \\
&= -\frac{1}{2} E^T Q\, E.
\end{aligned}$$

Thus, $V(t)$ is bounded for all time and, accordingly, $E, \tilde{\mu}_i, \tilde{D}_i \in L_\infty$, $1 \le i \le 3$. This exactly yields $\hat{\mu}_i, \hat{D}_i \in L_\infty$. Furthermore, we have $E \in L_\infty$ from the inequality of $\dot{V}$. When Assumption 3.2 holds as well, $\dot{\hat{\mu}}_i, \dot{\hat{D}}_i \in L_2 \cap L_\infty$ follows from the parameter adaptation law. Also, we can have $\dot{E} \in L_\infty$. This means the uniform continuity of E. Combining this with L_2 - property of E, we can use Barbalat's lemma to conclude that E converges to zero asymptotically. Also, from the parameter adaptation law, $\dot{\hat{\mu}}_i$ and $\dot{\hat{D}}_i$ converge to zero asymptotically. (Q.E.D.)

As the switching term is not desirable for practical application due to chattering phenomenon, a saturation function is used here. So, the nonlinear observer in Equation (11) and the adaptive law in Equation (12) are modified as

$$\begin{aligned}
\dot{\hat{X}} &= \begin{pmatrix} 0 & 1 & 0 \\ 0 & 0 & 1 \\ 0 & 0 & 0 \end{pmatrix} \hat{X} + \begin{pmatrix} k_1 \\ k_2 \\ k_3 \end{pmatrix} \varepsilon + \begin{pmatrix} m_1 \tilde{x}_1 \\ m_2 \tilde{x}_2 \\ m_3 \tilde{x}_3 \end{pmatrix} + \begin{pmatrix} 0 \\ 0 \\ -\hat{b}_g b_c \end{pmatrix} u_c \\
&\quad + \begin{pmatrix} 0 \\ 0 \\ -\hat{a}_{g1} x_2 - \hat{a}_{g2} x_3 + \hat{b}_g a_{c1} x_{c1} + \hat{b}_g a_{c2} x_{c2} \end{pmatrix} \\
&\quad + \begin{pmatrix} (\hat{\mu}_1^T |\varphi_1| + \hat{D}_1) sat(\tilde{x}_1 / d_{w1}) \\ (\hat{\mu}_2^T |\varphi_2| + \hat{D}_2) sat(\tilde{x}_2 / d_{w2}) \\ (\hat{\mu}_3^T |\varphi_3| + \hat{D}_3) sat(\tilde{x}_3 / d_{w3}) \end{pmatrix}
\end{aligned} \tag{13}$$

$$\dot{\hat{\mu}}_{ij} = \gamma_{\mu i} |\tilde{x}_i| \cdot |\varphi_{ij}|, \; \dot{\hat{D}}_i = \gamma_{Di} |\tilde{x}_i|. \tag{14}$$

Stability and performance for the above observer can proceed as in Theorem 3.1 to have $\lim_{t \to \infty} |\tilde{x}_i(t)| \le d_{wi}$ where $1 \le i \le 3$, which is omitted here.

Using the estimated states and uncertainties of the nonlinear observer in Equations (13) and (14), the output or the rate of line-of-sight can be made to converge to zero by the following guidance law, which is based on [4].

$$\begin{aligned}
u_c = \frac{1}{\hat{b}_g b_c} [& k_s s + k_3 \varepsilon - \hat{a}_{g1} x_2 - \hat{a}_{g2} x_3 + \hat{b}_g a_{c1} x_{c1} \\
& + \hat{b}_g a_{c2} x_{c2} + \varepsilon_{f3} + a_s (\hat{x}_3 + k_2 \varepsilon + \varepsilon_{f2}) \\
& + b_s \{ \hat{x}_2 + k_1 \varepsilon + \varepsilon_{f1} + k_f (\hat{x}_1 - \hat{x}_{f1}) \} + m_f]
\end{aligned} \tag{15}$$

where $\hat{x}_{f1}$ and $\hat{M}_f$ are generated from $\dot{\hat{x}}_{f1} = \hat{x}_2 + k_1 \varepsilon + \varepsilon_{f1} + k_f (\hat{x}_1 - \hat{x}_{f1})$, $\dot{M}_f = m_f$, $m_f = -a_M M_f + a_M (D_f - M_f)$, and $D_f = k_1 \dot{\varepsilon} + \dot{\varepsilon}_{f1} + (a_s - k_f) \varepsilon_{f1} + (a_s k_f - k_f^2) \cdot (\hat{x}_1 - \hat{x}_{f1}) + k_f m_1 \tilde{x}_1 + k_f (\hat{\mu}_1^T |\varphi_1| + \hat{D}_1) sat(\tilde{x}_1 / d_{w1}) + m_2 \tilde{x}_2 + (\hat{\mu}_2^T |\varphi_2| + \hat{D}_2) sat(\tilde{x}_2 / d_{w2})$, $\dot{\varepsilon}_{f1} = -a_{f1} \varepsilon_{f1} + a_{f1} \{ m_1 \tilde{x}_1 + (\hat{\mu}_1^T |\varphi_1| + \hat{D}_1) sat(\tilde{x}_1 / d_{w1}) \}$, $\dot{\varepsilon}_{fi} = -a_{fi} \varepsilon_{fi} + a_{fi} \{ m_i \tilde{x}_i + (\hat{\mu}_i^T |\varphi_i| + \hat{D}_i) sat(\tilde{x}_i / d_{wi}) + k_{i-1} \dot{\varepsilon} \}$ where $2 \le i \le 3$, $s = \hat{x}_3 + k_2 \varepsilon + a_s (\hat{x}_2 + k_1 \varepsilon) + b_s \hat{x}_{f1} + M_f$ is a sliding surface, $k_f > 0$ is an observer gain, and $a_s, b_s, a_M, a_{f1}, a_{f2} > 0$ are design parameters. The stability analysis of the guidance law in Equation (15) is omitted.

4 Simulation results

This section presents simulation results for the proposed observer (13-14) and guidance law (15) for each yaw and pitch dynamics, which is evaluated for a missile-target interception under surface-air engagement scenarios, which depend on the conditions of the missile and the target. The miss distance and flight time are chosen as performance indices. The actual missile control system in [7] is employed in a closed-loop guidance and control simulation environment described in [5]. The magnitude and rate saturation of the guidance commands u_c are included as $|u_c| \le 40g$ and $|\dot{u}_c| \le 400g/\sec$. The performance of the proposed nonlinear adaptive guidance (NAG) law is compared with that of proportional navigation guidance (PNG) law. Design parameters of control loop in Equation (4) are $\xi = 0.7$ and $\omega_n = 15$. Also, those of observer in Equations (13) and (14) are $k_1 = 50$, $k_2 = 30$, $k_3 = 10$, $m_1 = m_2 = m_3 = 3$, $a_0 = 50$, $\gamma_{\mu 1} = \gamma_{\mu 2} = \gamma_{\mu 3} = 0.01$, $\gamma_{D1} = \gamma_{D2} = \gamma_{D3} = 1$, $d_{w1} = d_{w3} = 0.01$, $d_{w2} = 0.1$, and those of guidance law in Equation (15) are $a_s = 250$, $b_s = 1$, $k_s = 5$, $k_f = 50$, $a_M = 0.01$, $a_{f1} = 200$, $a_{f2} = 1$.

Here, we selected several scenarios shown in Table I, where the target initially travels at constant velocity with 200 $m/\sec$ and make step-changes in acceleration. Each vector component represents the value along the y and z axis, respectively. The control start time of the missile is 0.5 sec. Parameters in Equation (5) are chosen as $\hat{a}_{g1} = 0$, $\tilde{a}_{g1} = \ddot{R}/R$, $\hat{a}_{g2} = 2\dot{R}/R$, $\tilde{a}_{g2} = 0$, $\hat{b}_g = 1/R$, and $\tilde{b}_g = 0$ by assuming that only R and $\dot{R}$ are available. Table II compares the miss distances and flight time of PNG and NAG under each scenario. Although the estimated states and uncertainties from nonlinear observer are used in NAG, NAG exhibits better performance than PNG. Fig. 1 shows the acceleration commands and actual accelerations, and three-dimensional missile-target trajectories for PN guidance (PNG) and proposed guidance (NAG) for Scenario I in Table I. We also performed for other scenarios and we could see that in overall cases the proposed scheme have better performance over PNG.

5 Conclusion

We proposed a nonlinear observer for a nonlinear adaptive guidance law. The simulation results show that the nonlinear adaptive guidance law using a proposed nonlinear observer can perform as much as the one where all of states are assumed to be available. More rigorous design and analysis of the guidance law combined with the nonlinear observer needs to be done and can be pursued as a further study.

Acknowledgements

This work was supported by the visiting fellow program of UNSW@ADFA (The University of New South Wales at Australian Defence Force Academy), Post-doctoral Fellowship Program of Korea Science & Engineering Foundation (KOSEF), the Brain Korea 21 Project, and the Automatic Control Research Center (ACRC) in Seoul National University.

Scenario	I	II	III
First evasive time (sec.)	0	0	0
First evasive acceleration ($m/\sec^2$)	[4 -4]	[0 8]	[0 –10]
Second evasive time (sec.)	2	2	2.5
Second evasive acceleration ($m/\sec^2$)	[8 -8]	[–8 0]	[15 0]

(a) Target conditions

Scenario	I	II	III
Off-boresight angle (deg)	-30	0	45
Aspect angle (deg)	-90	90	180
Elevation angle (deg)	0	0	0
Azimuth angle (deg)	0	0	0
Initial relative distance (m)	2000	3000	1500
Initial relative altitude (m)	1300	2500	1000

(b) Target-Missile geometry

Table I. Scenarios for missile-target interception

Scenario	PNG		NAG	
	MD	FT	MD	FT
I	7.7048m	4.9505sec.	0.9144m	5.2700sec.
II	4.3244m	5.8085sec.	4.6008m	5.7530sec.
III	1.8637m	3.9255sec.	0.9996m	3.7305sec.

Table II. Performance of PNG and NAG
(MD: Miss Distance, FT: Flight Time)

References

[1] K. R. Babu, I. G. Sarma, K. N. Swamy, K. N., “Switched Bias Proportional Navigation for Homing Guidance Against Highly Maneuvering Target,” *Journal of Guidance, Control, and Dynamics*, Vol. 17, No. 6, pp. 1357-1363, (1994).

[2] S. Bezik, I. Rusnak, W. S. Gray, “Guidance of a Homing Missile via Nonlinear Geometric Control Methods,” *Journal of Guidance, Control, and Dynamics*, Vol. 18, No. 3, pp. 441-448, (1995).

[3] S. D. Brierley, R. Longchamp, “Application of Sliding Mode Control to Air-Air Interception Problem,” *IEEE Transactions on Aerospace and Electronic Systems*, Vol. 26, No. 2, pp. 306-325, (1990)

[4] J. Y. Choi, D. Chwa, H. P. Cho, “Nonlinear Adaptive Guidance Considering Target Uncertainties and Control

Loop Dynamics," *Proceedings of the American Control Conference*, Aringlington, pp. 506-511, (2001).

[5] J. Y. Choi, D. Chwa, M. S. Kim, "Adaptive Control for Feedback-Linearized Missiles with Uncertainties," *IEEE Transactions on Aerospace and Electronic Systems*, Vol. 36, No. 2, pp.467-481, (2000).

[6] J. R. Cloutier, J. H. Evers, J. J. Feeley, "Assessment of Air to Air Missile and Guidance Technology," *IEEE Control Systems Magazine*, Vol. 9, pp. 27-34, (1989).

[7] D. Chwa, J. Y. Choi, "New Parametric Affine Modeling and Control for Skid-to-Turn Missiles," *IEEE Transactions on Control Systems Technology*, Vol. 9, No. 2, pp. 335-347, (2001).

[8] J. H. Evers, J. R. Cloutier, C. F. Lin, W. R. Yueh, Q. Wang, "Application of Integrated Guidance and Control Schemes to a Precision Guided Missile," *Proceedings of the American Control Conference*, Chicago, Illinois, USA, pp. 3225-3230, (1992).

[9] I. J. Ha, S. Chong, "Design of a CLOS Guidance Law via Feedback Linearization," *IEEE Transactions on Aerospace and Electronic Systems*, Vol. 28, No. 1, pp. 51-62, (1992).

[10] J. Huang, C. F. Lin, "A Modified CLOS Guidance Law via Right Inversion," *IEEE Transactions on Aerospace and Electronic Systems*, Vol. 31, No. 1, pp. 491-495, (1995).

[11] C. F. Lin, E. Ohlmeyer, J. E. Bibel, S. Malyevac, "Optimal Design of Integrated Missile Guidance and Control," *1998 World Aviation Conference*, Anaheim, CA, AIAA-985519, (1998).

[12] C. F. Lin, Q. Wang, J. L. Speyer, J. H. Evers, J. R. Cloutier, "Integrated Estimation, Guidance, and Control System Design Using Game Theoretic Approach," *Proceedings of the American Control Conference*, Chicago, Illinois, pp. 3220-3224, (1992).

[13] H. J. Pastric, S. Setlzer, M. E. Warren, "Guidance Laws for Short Range Homing Missile," *Journal of Guidance, Control, and Dynamics*, Vol. 4, No. 2, pp. 98-108, (1981).

[14] S. H. Song, I. J. Ha, "A Lyapunov-like Approach to Performance Analysis of 3-Dimensional Pure PNG Laws," *IEEE Transactions on Aerospace and Electronic Systems*, Vol. 30, No. 1, pp. 238-247, (1994).

[15] C. D. Yang, H. Y. Chen, "Nonlinear H_∞ Robust Guidance Law for Homing Missiles," *Journal of Guidance, Control, and Dynamics*, Vol. 21, No. 6, pp. 882-890, (1998).

[16] D. Zhou, C. Mu, W. Xu, "Adaptive Sliding-Mode Guidance of a Homing Missile," *Journal of Guidance, Control, and Dynamics*, Vol. 22, No. 4, pp. 589-594, (1999).

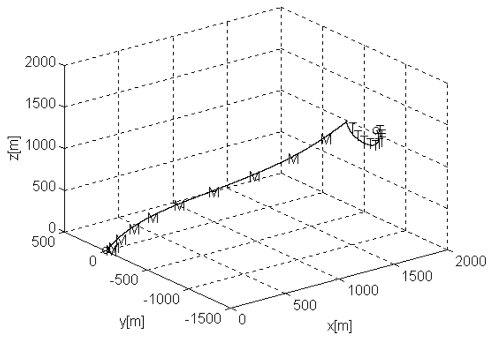

(a) acceleration of PNG

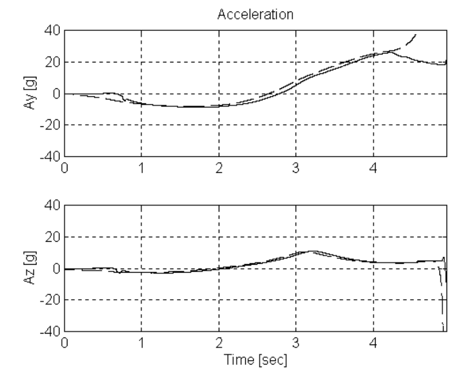

(b) trajectory of PNG

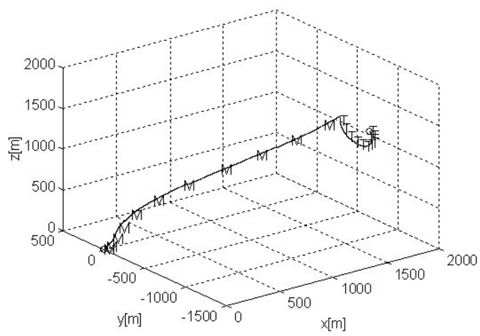

(c) acceleration of NAG

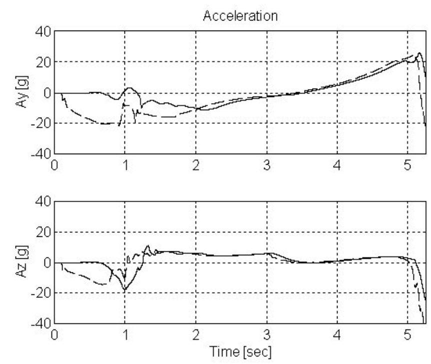

(d) trajectory of NAG

Fig. 1 Performance of Scenario I
(in (a),(c), Solid: actual acceleration, Dotted: acceleration command; in (b),(d), M: missile, T: target)